



## The effect of bilirubin on Bad, Bak, and Bim pro-apoptotic factors: A molecular dynamic simulation study

Javad Saffari-Chaleshtori<sup>1,2</sup>, Sayed Mohammad Shafiee<sup>2\*</sup> & Esfandiar Heidarian<sup>3</sup>

<sup>1</sup>Student Research Committee, Shiraz University of Medical Sciences, Shiraz, Iran

<sup>2</sup>Department of Biochemistry, School of Medicine, Shiraz University of Medical Sciences, Shiraz, Iran

<sup>3</sup>Clinical Biochemistry Research Center, Basic Health Sciences Institute, Shahrekord University of Medical Sciences, Shahrekord, Iran

Received 04 April 2020; revised 18 May 2021

Bilirubin, an endogenous catabolic product of the heme catabolism, can induce apoptosis in damaged cells. This study investigated the effect of bilirubin on three pro-apoptotic factors Bad, Bak, and Bim using docking and molecular dynamics simulation. Three-dimensional structures were obtained from PubChem and RCSB servers. The simulation was accomplished at 40 nanoseconds (ns) using GROMACS 2018 simulation package before docking. Then bilirubin, as a ligand, bound to these proteins by Autodock v.4.2.6 software, and molecular dynamics simulation were performed again. The hydrophobic and hydrogen bonds at the binding site were determined using LigPlot<sup>+</sup>V.4.5.3 software. Our study revealed that bilirubin has the highest tendency to bind the Bim. This binding occurred between the 10 residues at the Bim binding site with the lowest binding energy (-8.43 kcal/mol). The docking of bilirubin to Bad, Bak, and Bim decreased Total Energy (TE), increased Radius of gyration (Rg), and root-mean-square deviation (RMSD). The coil secondary structures of Bad and Bim increased significantly after docking the bilirubin. Due to exhibiting a high tendency to interact with Bad, Bak, and Bim, bilirubin can affect their molecular dynamics and increase their activity so that, apoptosis is induced in the cell, which is considered in cancer treatment.

**Keywords:** Apoptosis, Hetero-oligomerization, Homo-oligomerization, Protein conformation, Three-dimensional structure

Bilirubin is a tetrapyrrole and an endogenous catabolic product that is formed during heme catabolism<sup>1</sup>. After lysis of the erythrocytes in the spleen and liver, macrophages remove the hemoglobin and separate the heme group. Subsequently, hemeoxygenase converts the heme to biliverdin that is converted to unconjugated bilirubin by the biliverdin reductase enzyme. Unconjugated bilirubin combines with glucuronic acid to form conjugated bilirubin in the liver and is then excreted in bile. The normal level of (unconjugated) bilirubin under physiological conditions is around 0.2 mg/dL (3.42  $\mu$ M)<sup>2</sup>. Bilirubin is a lipophilic compound and tends to cross the blood- brain barrier<sup>3</sup>. This compound, at high concentrations, can exert neurotoxic effects and therefore induce severe complications in neurons<sup>4</sup>. Neonatal jaundice is the most common cause of bilirubinemia. The genetic causes of this condition include Gilbert-Meulengracht, Crigler-Najjar, and Rotor syndrome<sup>2</sup>. Serum bilirubin concentrations are

lower than 12-14 mg/dL are tolerable while higher levels lead to mental retardation especially in neonates<sup>5</sup>. However, a mutation in theuridine 5'-diphosphoglucuronosyltransferase (*UDP-glucuronosyltransferase*, UGT) gene causes a natural increase in bilirubin up to 1-3 mg/dL (17-51  $\mu$ M) in Gilbert-Meulengracht syndrome<sup>6</sup>.

Serum bilirubin levels increase in certain diseases such as gallstones and pancreatic cancer<sup>7</sup>. Some studies, however, have shown that increased serum bilirubin concentration can protect against certain cancers<sup>8</sup>. Patients with Gilbert-Meulengracht syndrome are less susceptible to cancer<sup>9,10</sup>. Bilirubin is the most important antioxidant endogenous cytoprotectant due to two hydroxyl groups in its structure. Because of its continuous recycling in the bilirubin-biliverdin redox cycle, bilirubin may also be the most potent endogenous antioxidant<sup>11</sup>. About 10% of the total antioxidant capacity in adults is related to bilirubin<sup>8</sup>. In some cancers such as lung cancer, the range of bilirubin levels has been reported to decrease significantly<sup>12</sup>.

Bilirubin induces apoptosis by exerting an effect on mitochondria, releasing cytochrome *c* (Cyt *c*) into the cytosol, and activating caspase-9<sup>13</sup>. The pro-apoptotic

\*Correspondence:

Phone: +98 (71) 32303029;

Fax: +98 (71) 32303029

E-mail: shafieem@sums.ac.ir

factors Bad, Bak, and Bim are the members of the Bcl-2 family which induce apoptosis by increasing the cellular caspases activity and releasing Cyt *c* into the cytosol by affecting mitochondria<sup>14,15</sup>. Activation of These pro-apoptotic factors led to initiate the apoptosis trigger<sup>16</sup>. Bcl-2 family proteins interact with downstream proteins and activate the apoptotic cascade pathways. The affinity between the partners is the result of changes in protein conformation that determine the amount of interaction between them<sup>17</sup>. Bad, a main pro-apoptotic member of the Bcl-2 family, interacts with anti-apoptotic factors and induces apoptosis in damaged cells<sup>18</sup>. Another pro-apoptotic factor, Bak, can form homo-oligomerization or hetero-oligomerization on mitochondria to directly cause mitochondrial outer membrane permeability (MOMP) and induce the intrinsic apoptotic pathway<sup>19</sup>. Bim pro-apoptotic factor, a Bcl-2 family cell survival regulator, has the main role in inducing the mitochondrial depolarization and activating the apoptosis<sup>20</sup>.

Compounds with apoptosis-inducing effects are highly used for many purposes in the treatment of some cancers<sup>21</sup>. Bilirubin can induce serious damage to cells by activating apoptosis. Therefore, it can use to inhibit or treat cancer cells as a candidate compound. This simulation study investigated the tendency of bilirubin, as an endogenous antioxidant, to interact with the pre-apoptotic factors Bad, Bak, and Bim that plays an important role in the apoptotic process as well as the molecular dynamic effects of bilirubin on these factors.

## Materials and Methods

### PDB files Preparation

The Bad, Bak, and Bim pro-apoptotic PDB files were obtained from the protein data bank server ([www.rcsb.org](http://www.rcsb.org)) with protein data bank (PDB) ID (Bad ID:1G5J, BakID:1BXL, and BimID:1PQ1).The inhibitor, ions, and water molecules were removed, and the proteins were used as a template structure and were displayed using Arguslab software V.4.0.1. Then, the three-dimensional structure of the bilirubin file was obtained from the Pubchem server ([www.pubchem.ncbi.nlm.nih.gov](http://www.pubchem.ncbi.nlm.nih.gov)) and then optimized and converted to PDB file by ArguslabV.4.0.1 software.

### Molecular dynamics (MD) simulation of Bad, Bak, and Bim

The molecular dynamics simulation of the Bad, Bak, and Bim structures were first investigated in pure water. The force field of G43A1 with SPC216 model was used for protein-ligand interaction

simulation between the three pro-apoptotic factors and bilirubin<sup>22</sup>. The GROMACS 2018 simulation package was used to analyze the molecular dynamic parameters. Three Grid Boxes with suitable ( $x \times y \times z$  nm) parameters (Bad; 5.2×5.2×3.7 nm, Bak; 4.6×4.6×3.3 nm, and Bim; 3.3×3.3×2.3 nm) were designed for each protein. By calculation of the electrical charge of each protein, appropriate amounts of sodium and chloride were used to neutralize the molecules to prepare 140 mM concentration of Na<sup>+</sup> and Cl<sup>-</sup> in water for each protein<sup>23</sup>. The energy of the systems was minimized through 40000 steps (40 nanoseconds (ns) by steepest descent method, and equilibrated for 2 ns in the NVT ensemble. The temperature was set at 300K for all the simulation intervals. Then, the output PDB file was used as an input molecular docking structure to simulate complexes.

### Molecular docking

Docking studies were done by Autodock V.4.2.6 to assign Gasteiger partial charges to each atom of the proteins in the PDB format. Molecular docking of bilirubin with Bad, Bak, and Bim was used to identify the best sites of ligand-receptor bonds and to determine the most stable free energy of ligand-receptor. In this study, three Grid Boxes (Bad; 5.2×5.2×3.7 nm, Bak; 4.6×4.6×3.3 nm, and Bim; 3.3×3.3×2.3 nm) were used to generate grid parameter file (gpf) and a docking parameter file (dpf). Then, these files were used as input files for grid mapping and docking, respectively. After the production of PDBQ and PDBQT files, the PDBQT file of bilirubin was considered as ligand and the PDBQT files of Bad, Bak, and Bim were considered as receptors. The *autogrid4 -p n.gpf -l n.gle* linux order code was used to produce the n.gle text file. Two hundred independent runs were performed for each ligand and the distinct conformers generated were docked randomly into the binding pocket of these proteins. Genetic algorithm (GA) and Lamarckian GA parameters were used for ligand conformational search in this docking study. The *autodock4 -p n.dpf -l n.dlg* linux order code was used to produce the n.dlg text file. All data obtained from n.dlg files were analyzed and used in the following investigations<sup>24</sup>.

In this study, the LigPlot<sup>+</sup>V.4.5.3 software was used to determine the number of hydrophobic and hydrogen bonds between bilirubin and Bad, Bak, and Bim in the binding sites. The type and number of amino acids presented in the binding site were also determined by LigPlot<sup>+</sup>V.4.5.3 software<sup>25</sup>.

### MD simulation of Bad, Bak, and Bim with bilirubin

Finally, the molecular dynamics simulation of the Bad, Bak, and Bim pro-apoptotic proteins, as receptors, was performed with bilirubin, as a ligand, and parameterization was performed using PRODRG server in 140 mM concentration of Na<sup>+</sup> and Cl<sup>-</sup> in water in accordance with the above method. As already explained, the paths stored in the simulation were used to analyze the structural parameters of the complex. The results of simulation of the Bad, Bak, and Bim molecules with and without ligand were comparatively analyzed using the Grapher v.15 software<sup>26</sup>.

### Statistical analysis

The data was analyzed by the SPSS V.22 (Chicago, IL, USA). A paired sample *t*-test was performed to analyze molecular dynamics. *P*<0.001 was considered a significance level.

### Results

The binding energy (BE), final intermolecular energy (FIE), estimated inhibition constant (EIC), and the number of intermolecular interactions such as hydrogen bonds and hydrophobic bonds between the bilirubin and Bad, Bak, and Bim are shown in (Table 1).

Figure 1 shows a three-dimensional position and interaction (hydrogen and hydrophobic) bonds between bilirubin and Bad, Bak, and Bim pro-apoptotic residues.

The amounts of root mean-square deviation (RMSD) in the simulation of Bad, Bak, and Bim alone as well as in the simulation of Bad, Bak, and Bim in complex with bilirubin at 40 ns of the simulation are shown in (Fig. 2). At the first simulation, unstable conditions were observed until 10 ns. But, the pro-apoptotic proteins Bad, Bak, and Bim became stable at the end of 40 ns of simulation in RMSD.

Figure 3 shows the amount of Total Energy (TE) in the simulation of Bad, Bak, and Bim alone as well as that of Bad, Bak, and Bim in complex with bilirubin at 40 ns of simulation.

The amounts of Radius of gyration (Rg) in the simulation of Bad, Bak, and Bim alone (black) and in complex with bilirubin (red) at 40 ns of the simulation are illustrated in (Fig. 4).

In this simulation study, the mean fluctuations for all the residues of Bad, Bak, and Bim pro-apoptotic factors were investigated by the root mean square fluctuation (RMSF) (Fig. 5 & Table 2). After docking, the mean RMSF of the bilirubin-Bad and bilirubin-Bak complexes

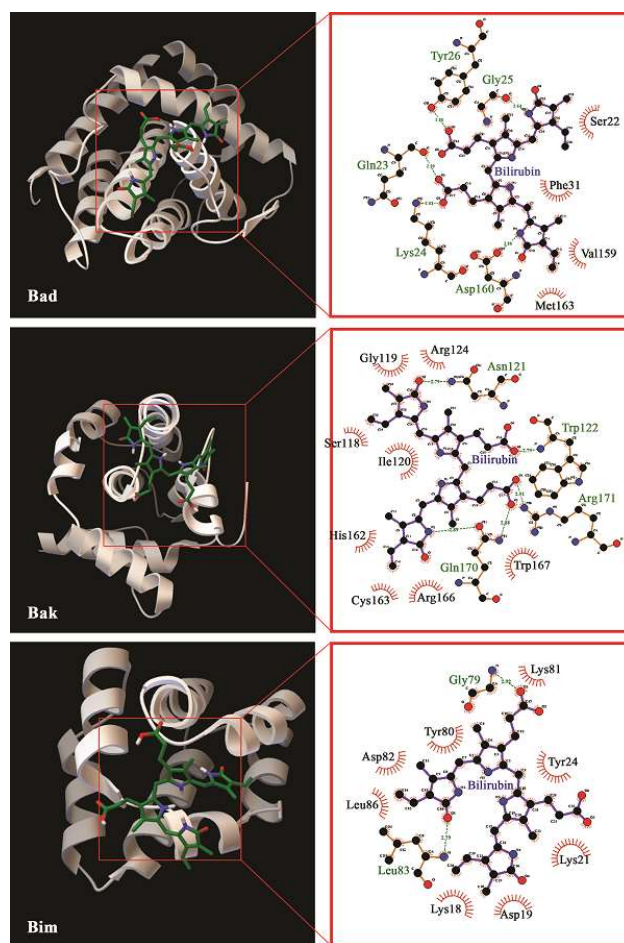


Fig. 1 — Display the three-dimensional position of bilirubin docked on receptors Bad, Bak, and Bim and shows the protein–ligand interactions in binding site residues

Table 1 — Inter molecular interactions between bilirubin with Bad, Bak, and Bim

Ligand- receptor	BE kcal/mol	FIE kcal/mol	EIC (Ki) $\mu$ M	Hydrogen Bonds	Hydrophobic Bonds
Bilirubin-Bad	-7.28	-11.45	4.63	Gln23, Lys24, Gly25, Tyr26, Asp160	Ser22, Phe31, Val59, Met163
Bilirubin-Bak	-6.92	-11.09	8.51	Asn121, Trp122, Gln170, Arg171	Ser118, Gly119, Ile120, Arg124, His162, Cys163, Arg166, Trp167
Bilirubin-Bim	-8.43	-12.61	0.66	Gly79, Leu83	Lys18, Asp19, Lys21, Tyr24, Lys81, Tyr80, Asp82, Leu86

Abbreviations: BE; Estimated Free Energy of binding (kcal/mol), FIE; final intermolecular energy (kcal/mol), EIC; estimated inhibition constant ( $\mu$ M)

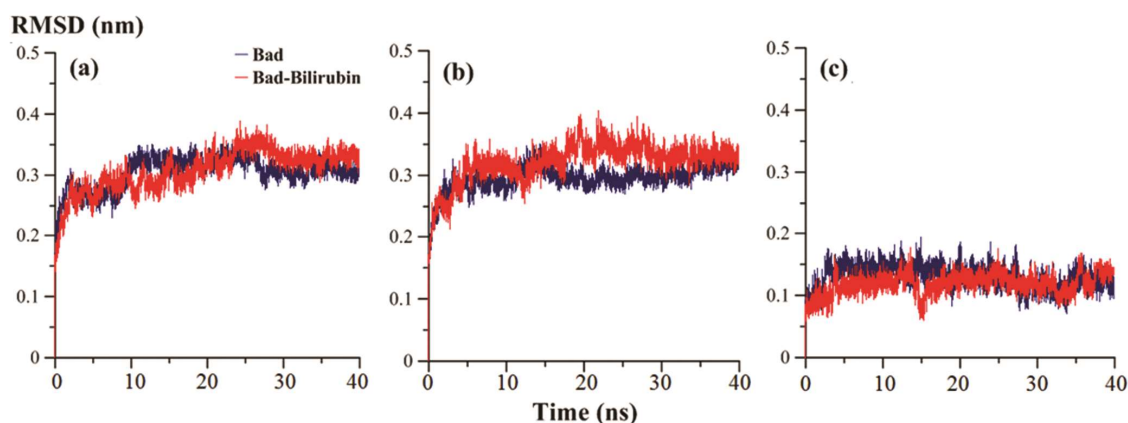


Fig. 2 — Root mean-square deviation (RMSD) for (A) Bad; (B) Bak; and (C) Bim alone (black) and in complex with bilirubin (red). Statistical analysis was done by independent sample *t*-test. Each point represents mean  $\pm$  SD. Difference between the red and black lines was significant ( $P < 0.001$ )

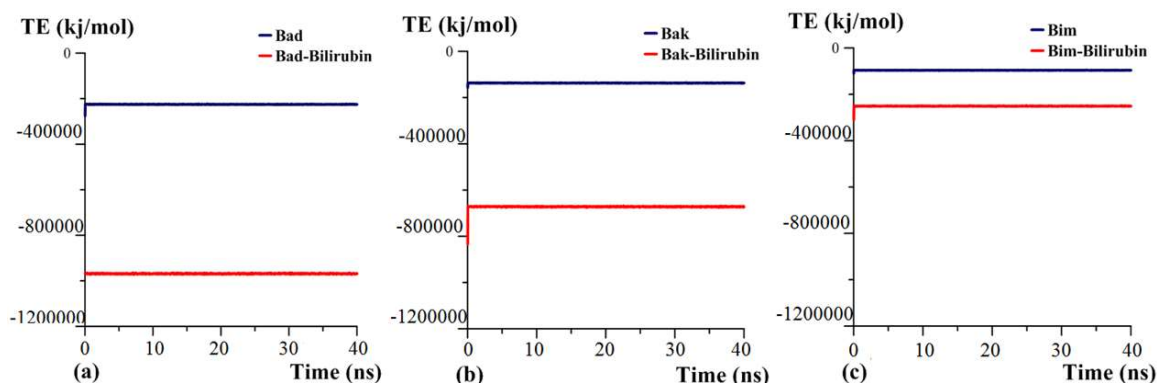


Fig. 3 — Total Energy (TE) for (A) Bad; (B) Bak; and (C) Bim alone (black) and in complex with bilirubin (red). Statistical analysis was done by independent sample *t*-test. Each point represents mean  $\pm$  SD. Difference between the red and black line was significant ( $P < 0.001$ )

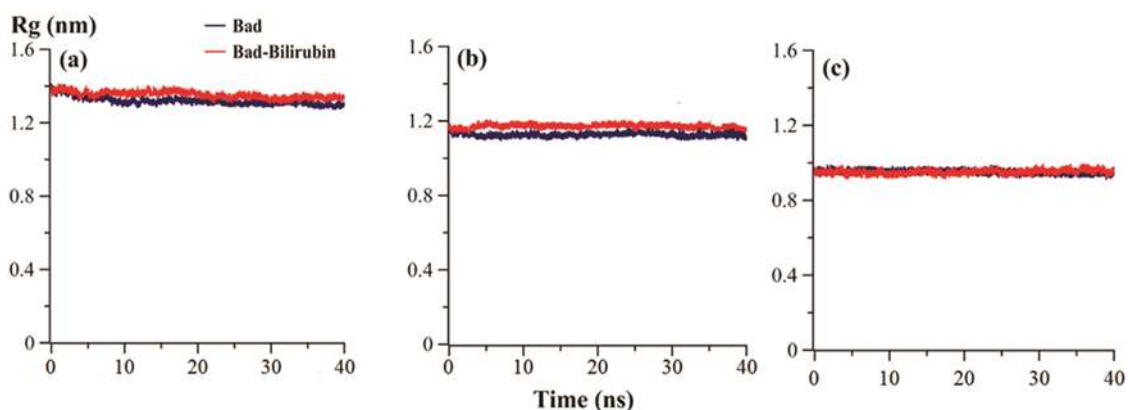


Fig. 4 — Radius of gyration (Rg) for (A) Bad; (B) Bak; and (C) Bim alone (black) and in complex with bilirubin (red). Statistical analysis was done by independent sample *t*-test. Each point represents mean  $\pm$  SD. Difference between the red and black line was significant ( $P < 0.001$ )

decreased but the mean RMSF of the bilirubin-Bim complex significantly increased.

Molecular dynamic parameters such as TE, RG, RMSD, RMSF, and ASA in simulation of Bad, Bak, and Bim alone as well as in simulation of Bad, Bak,

and Bim in complex with bilirubin at 40 ns of the simulation are shown in (Table 2).

Variations in the secondary structure of Bad, Bak, and Bim pro-apoptotic proteins, as agents to predict the protein structure and activity in complex with

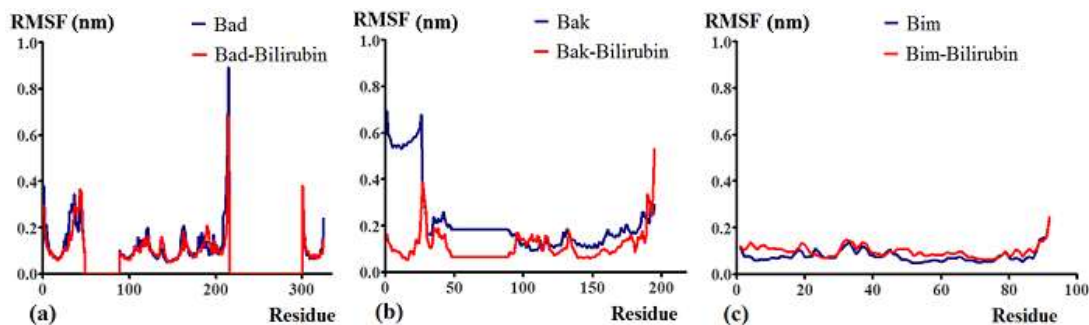


Fig. 5 —Root mean square fluctuation (RMSF) for (A) Bad; (B) Bak; and (C) Bimalone (black) and in complex with bilirubin (red). Statistical analysis was done by independent sample *t*-test. Each point represents mean  $\pm$  SD. Difference between the red and black line was significant ( $P < 0.001$ )

Table 2 — Molecular dynamics simulation parameters

Parameters	RMSD	TE	RG	RMSF	ASA
Bad	0.30 (0.03)	-226592 (1353.3)	1.32 (0.02)	0.13 (0.10)	0.52 (0.12)
Bad-bilirubin	0.31 (0.03)*	-969508 (5346)*	1.35 (0.18)*	0.12 (0.08)*	0.53 (0.12)*
Bak	0.29 (0.02)	-136006 (731.1)	1.14 (0.09)	0.23 (0.16)	0.53 (0.12)
Bak-bilirubin	0.33 (0.03)*	-672904 (3789)*	1.17 (0.01)*	0.12 (0.07)*	0.54 (0.12)*
Bim	0.13 (0.18)	-95022.8 (565)	0.95 (0.01)	0.08 (0.03)	0.52 (0.11)
Bim-bilirubin	0.12 (0.17)*	-251387 (1501)*	0.95 (0.01)	0.10 (0.03)*	0.52 (0.11)

The amounts of molecular dynamics simulation parameters such as TE, RG, RMSD, and RMSF for Bad, Bak, and Bim alone and in complex with bilirubin at 40 ns of simulation. Statistical analysis was conducted by independent sample *t*-test. Each point represents mean  $\pm$  SD. \*Differences between the Bad, Bak, and Bim alone and Bad, Bak, and Bim complexes with bilirubin were significant ( $P < 0.001$ )

Table 3 — Secondary structure of receptors and receptors-ligand complexes

Protein-ligand	Coil (%)	$\beta$ -Sheet (%)	$\alpha$ -Helix (%)
Bad	42.3	9.1	48.6
Bad-bilirubin	44.2*	8.1*	47.7*
Bak	40.8	13.2	46.0
Bak-bilirubin	40.5	12.8	46.7
Bim	50.7	0	49.3
Bim-bilirubin	51.6*	0	48.4*

The Secondary structure variation such as Coil,  $\beta$ -Sheet, and  $\alpha$ -Helix of Bad, Bak, and Bim alone and in complex with bilirubin at 40 ns of simulation. Statistical analysis was done by Independent sample *t*-test. Each point represents mean  $\pm$  SD. \*Difference between the Bad, Bak, and Bim alone, and Bad, Bak, and Bim complexes with bilirubin were significant ( $P < 0.001$ )

bilirubin at 40 ns of the simulation, are shown in (Table 3).

## Discussion

Our results showed that bilirubin had a great tendency to bind the Bad, Bak, and Bim pro-apoptotic proteins. The tendency of bilirubin to bind to the Bim protein is higher than that to bind the Bad and Bak proteins, evident from more BE being released from Bim than the other two proteins (Table 1). The hydrogen and hydrophobic bonds between the bilirubin and proteins in binding sites (Table 1 &

Fig. 1) confirm the high tendency of bilirubin to interact with Bad, Bak, and Bim. Our study showed that the interaction between the bilirubin and Bad, Bak, and Bim proteins is much stronger than that to bind gallic acid<sup>26</sup>, carvacrol<sup>27</sup>, and quercetin<sup>28</sup>, to the Bad, Bak, and Bim proteins. The most important point is the lowest concentration of bilirubin for binding to the sites. The bilirubin EIC (Table 1) for binding to Bad, Bak, and Bim was much lower than the IC<sub>50</sub> needed for inducing apoptosis in certain cancer cells line<sup>29,30</sup>. These results show that bilirubin at average concentrations (relatively higher than normal range) can bind to these pro-apoptotic proteins in these conditions; bilirubin can induce molecular dynamic effects on these proteins, and therefore is more likely to be active and to bind to downstream factors and induce the cell apoptotic pathways.

The results of this study showed that the RMSD increased for all the complexes after docking the bilirubin with Bad, Bak, and Bim. However, the RMSD of bilirubin-Bim complex decreased substantially and became unstable at the completion of 40 ns (Fig. 2 & Table 2). The RMSD changes of Bad, Bak, and Bim in the present of bilirubin showed a tendency for changes in their backbone<sup>31</sup>.

Some molecular dynamic simulation studies have been used to identify the anti-cancer effects of compounds that interact with pro-apoptotic and anti-apoptotic factors as activators and inhibitors, respectively<sup>32,33</sup>.

The highest amount of TE released from ligand-receptors was obtained for the Bad-bilirubin complex ( $\Delta G = -742881$  KJ/mol) (Fig. 3 & Table 2). This shows that although bilirubin has a favorable tendency to interact with all three molecules, the Bad molecule, when binding to bilirubin, is more reactive compared to the Bak and Bim molecules<sup>26</sup>. The results regarding Rg showed that all three molecules were stable during the simulation period. These results showed that changes in the Rg amount of unbound Bim molecule are very small and not significant in comparison with those in the Rg amount of the Bim-bilirubin complex, but the Rg of bilirubin-Bad and bilirubin-Bak complexes increased compared to those of the Bad and Bak molecules (Fig. 4 & Table 2). An increase in the amount of Rg increases the likelihood of access to the protein active site, which may increase the activity of the protein<sup>34</sup>. Therefore this change in Rg predicts an increase in Bad and Bak activity after docking the bilirubin. The RMSF results (Fig. 5 & Table 2) show that bilirubin can increase the activity of the Bim molecule by increasing the fluctuations of its residues and increasing RMSF. The binding of bilirubin to the Bad and Bak pro-apoptotic proteins leads to a significant increase in accessible surface area (ASA). But, there is no change in ASA in the binding of bilirubin to the Bim pro-apoptotic protein (Table 2). Therefore, an increase in ASA leads to a decrease in the hydrophobicity of Bad and Bak proteins that can interact with other Bcl-2 family pro-apoptotic factors and inducing apoptosis<sup>35</sup>.

This simulation study showed an increase in the coil structures of Bad and Bim molecules and a decrease in their alpha and beta structures. Since the active site of proteins exist in turn or coil structures, after docking the bilirubin with the Bad and Bim molecules (Bad-bilirubin and Bim-bilirubin complexes) the amount of active and reactive sites increased in the Bad and Bim molecules, leading to an increase in interaction with other pro-apoptotic factors of Bcl-2 family and induction of apoptosis.

Some anticancer drugs induce apoptosis in cancer cells *via* direct interaction with pro-apoptotic factors and change in the conformational structures which result

inactivation of the homologous and heterologous pro-apoptotic factors dimers<sup>36,37</sup>. The results of this study showed that bilirubin could activate apoptosis by exerting the effects of molecular dynamics on the three pre-apoptotic molecules. These effects such as increase in Rg and ASA or increase in coil and turn secondary structures, lead to an increase in the regions of binding site for binding to other pro-apoptotic factors of Bcl-2 family and inducing apoptosis. These conformational changes lead to regulation and induction of pro-apoptotic factors dimerization<sup>38,39</sup>. This leads to mitochondrial permeabilization and induction of apoptosis<sup>40</sup>.

Some studies have shown that bilirubin can induce apoptosis in cancer cells, such as colon cancer, ductal carcinoma, hepatocellular carcinoma, and pancreas carcinoma<sup>13,29,30</sup>. Ollinger *et al.* observed that bilirubin inhibited the growth of HRT-18 colon cancer cell line by activating the mitogen-activated protein kinase/extracellular-signal-regulated kinase (MEK/ERK) pathway and induced apoptotic factors<sup>30</sup>. Keshavan *et al.* reported that bilirubin can lead to cell arresting in G1 phase and induce apoptosis by increasing the release of Cyt *c* from mitochondria<sup>13</sup>. Yuan *et al.* observed that bilirubin could induce apoptosis by increasing P38 and caspase 3 activities and decreasing Bcl-2 activity<sup>41</sup>. In some studies, bilirubin has been used to prepare nanoparticles that can specifically transport small molecules and anticancer drugs to cellular targets in cancer pharmacotherapy<sup>42,43</sup>. This study predicts that the apoptotic properties of bilirubin could be due to its molecular dynamics-related effects on pre-apoptotic proteins.

## Conclusion

Bilirubin can change the molecular dynamics of the Bad, Bak, and Bim pro-apoptotic factors due to exhibiting high tendency to interact with them through hydrogen and hydrophobic bonds. This study showed that among the three pro-apoptotic factors (Bad, Bak, and Bim), the Bad pro-apoptotic factor have more pronounced changes in Rg, RMSF, and TE and increasing the coil structure after docking with bilirubin. These changes can increase its activity and induce apoptosis in cells, which is very important to decrease cancer cell proliferation and therefore is useful for cancer treatment.

## Acknowledgement

This study was funded by the Deputy of Research and Technology of the Shiraz University of Medical

Sciences, Shiraz, Iran, based on the research project number: 19900. The results described in this paper were the Ph.D dissertation of Mr. Javad Saffari-Chaleshtori.

### Conflict of interest

All authors declare no conflict of interest.

### References

- Hansen TW, Wong RJ & Stevenson DK, Molecular Physiology and pathophysiology of bilirubin handling by the blood, liver, intestine, and brain in the newborn. *Physiol Rev*, 100 (2020) 1291.
- Burtis CA, Ashwood ER & Bruns DE, *Tietz textbook of clinical chemistry and molecular diagnostics-e-book* (Elsevier Health Sciences) 2012, 776.
- Cayabyab R & Ramanathan R, High unbound bilirubin for age: a neurotoxin with major effects on the developing brain. *Pediatr Res*, 85 (2019) 183.
- Ye H, Xing Y, Zhang L, Zhang J, Jiang H, Ding D, Shi H & Yin S, Bilirubin-induced neurotoxic and ototoxic effects in rat cochlear and vestibular organotypic cultures. *Neurotoxicol*, 71 (2019) 75.
- Schwertner HA & Vitek L, Gilbert syndrome, UGT1A1\* 28 allele, and cardiovascular disease risk: possible protective effects and therapeutic applications of bilirubin. *Atherosclerosis*, 198 (2008) 1.
- Wu X, Zhou D, Song J, Sun M & Pan Y, Molecular probes for identification of UDP-glucuronosyltransferase 1 gene polymorphisms for Gilbert's syndrome diagnosis. *Biomed Res*, 29(2018) 2111.
- Álvarez R, Carrato A, Adeva J, Alés I, Prados S, Valladares M, Macarulla T, Muñoz A & Hidalgo M, Management of hyperbilirubinaemia in pancreatic cancer patients. *Eur J Cancer*, 94 (2018) 26.
- Zucker SD, Horn PS & Sherman KE, Serum bilirubin levels in the US population: gender effect and inverse correlation with colorectal cancer. *J Hepatol*, 40 (2004) 827.
- Claridge LC, Armstrong MJ, Booth C & Gill PS, Gilbert's syndrome. *BMJ*, 342 (2011) d2293.
- King D & Armstrong M, Overview of Gilbert's syndrome. *Drug Ther Bull*, 57 (2019) 27.
- Sedlak TW, Saleh M, Higginson DS, Paul BD, Juluri KR & Snyder SH, Bilirubin and glutathione have complementary antioxidant and cytoprotective roles. *Proc Natl Acad Sci U S A*, 106 (2009) 5171.
- Lim JE, Kimm H & Jee SH, Combined effects of smoking and bilirubin levels on the risk of lung cancer in Korea: The Severance Cohort Study. *PLoS One*, 9 (2014) 103972.
- Keshavan P, Schwemberger SJ, Smith DL, Babcock GF & Zucker SD, Unconjugated bilirubin induces apoptosis in colon cancer cells by triggering mitochondrial depolarization. *Int J Cancer*, 112 (2004) 433.
- Engel T & Henshall DC, Apoptosis, Bcl-2 family proteins and caspases: the ABCs of seizure-damage and epileptogenesis. *Int J Physiol*, 1 (2009) 97.
- Wen X, Lin ZQ, Liu B & Wei YQ, Caspase-mediated programmed cell death pathways as potential therapeutic targets in cancer. *Cell Prolif*, 45 (2012) 217.
- Kazi A, Sun J, Doi K, Sung SS, Takahashi Y, Yin H, Rodriguez JM, Becerril J, Berndt N, Hamilton AD & Wang HG, The BH3  $\alpha$ -helical mimic BH3-M6 disrupts Bcl-XL, Bcl-2, and MCL-1 protein-protein interactions with Bax, Bak, Bad, or Bim and induces apoptosis in a Bax-and Bim-dependent manner. *J Biol Chem*, 286 (2011) 9382.
- Kale J, Osterlund EJ & Andrews DW, BCL-2 family proteins: changing partners in the dance towards death. *Cell Death Differ*, 25 (2018) 65.
- Liu Z, Zhang G, Huang S, Cheng J, Deng T, Lu X, Adeshakin FO, Chen Q & Wan X, Induction of apoptosis in hematological cancer cells by dorsomorphin correlates with BAD upregulation. *Biochem Biophys Res Commun*, 522 (2020) 704.
- Wang Y, Su W, Mai Z, Du M, Yu S, Liu Y, Wang X & Chen T, Co-expression of Mcl-1 and Bcl-2 induces mitochondrial swelling. *Biochem Biophys Res Commun*, 527 (2020) 866.
- Ludwig LM, Roach LE, Katz SG & LaBelle JL, Loss of BIM in T cells results in BCL-2 family BH3-member compensation but incomplete cell death sensitivity normalization. *Apoptosis*, 28 (2020) 1.
- Gayle SS, Sahni JM, Webb BM, Weber-Bonk KL, Shively MS, Spina R, Bar EE, Summers MK & Keri RA, Targeting BCL-xL improves the efficacy of bromodomain and extraterminal protein inhibitors in triple-negative breast cancer by eliciting the death of senescent cells. *J Biol Chem*, 294 (2019) 875.
- Nasab RR, Mansourian M, Hassanzadeh F & Shahlaei M, Exploring the interaction between epidermal growth factor receptor tyrosine kinase and some of the synthesized inhibitors using combination of *in silico* and *in vitro* cytotoxicity methods. *Res Pharm Sci*, 13 (2018) 509.
- Project E, Nachliel E & Gutman M, Force field-dependant structural divergence revealed during long time simulations of Calbindin d9k. *J Comput Chem*, 31 (2010) 1864.
- Morris GM, Goodsell DS, Halliday RS, Huey R, Hart WE, Belew RK & Olson AJ, Automated docking using a Lamarckian genetic algorithm and an empirical binding free energy function. *J Comput Chem*, 19 (1998) 1639.
- Saffari-Chaleshtori J, Heidari-Sureshjani E, Moradi F & Heidarian E, The Effects of Thymoquinone on Viability, and Anti-apoptotic Factors (BCL-XL, BCL-2, MCL-1) in Prostate Cancer (pc3) cells: an *in vitro* and computer-Simulated Environment Study. *Adv Pharm Bull*, 9 (2019) 490.
- Saffari-Chaleshtori J, Heidari-Sureshjani E, Moradi F, Jazi HM & Heidarian E, The study of apoptosis-inducing effects of three pre-apoptotic factors by gallic acid, using simulation analysis and the comet assay technique on the prostatic cancer cell line PC3. *Malays J Med Sci*, 24 (2017) 18.
- Saffari Chaleshtori J, Heidari-Soureshjani E, Reisi F, Tabatabaiefar MA, Asadi-Samani M, Zamanian N & Bahmani M, Damage intensity of carvacrol on prostatic cancer cells line Du145 and molecular dynamic simulation of it effect on apoptotic factors. *Int J Pharm Tech Res*, 9 (2016) 261.
- Saffari-Chaleshtori J, Heidari-Soureshjani E & Asadi-Samani M, Computational study of quercetin effect on pre-apoptotic factors of Bad, Bak and Bim. *J Herb Med Pharmacol*, 5 (2016) 61.
- Rao P, Suzuki R, Mizobuchi S, Yamaguchi T & Sasaguri S, Bilirubin exhibits a novel anti-cancer effect on human adenocarcinoma. *Biochem Biophys Res*, 342 (2006) 1279.
- Ollinger R, Kogler P, Troppmair J, Hermann M, Wurm M, Drasche A, Konigsrainer I, Amberger A, Weiss H, Ofner D

- & Bach FH, Bilirubin inhibits tumor cell growth via activation of ERK. *Cell Cycle*, 6 (2007) 3078.
- 31 Bell EW & Zhang Y, Dock RMSD: an open-source tool for atom mapping and RMSD calculation of symmetric molecules through graph isomorphism. *J Cheminformatics*, 11 (2019)40.
- 32 Anantram A, Kundaikar H, Degani M & Prabhu A, Molecular dynamic simulations on an inhibitor of anti-apoptotic Bcl-2 proteins for insights into its interaction mechanism for anti-cancer activity. *J Biomol Struct Dyn*, 37 (2019) 3109.
- 33 Arpudhamary V, Priya S, Manzoor MA, Mubarakali D & Hemalatha S, Apoptotic-inducing factor 1 (AIF1) plays a critical role in cembranoid mediated apoptosis to control cancer: Molecular docking and dynamics study. *Biocatal Agric Biotechnol*, 22 (2019) 101343.
- 34 Lobanov MY, Bogatyreva N & Galzitskaya O, Radius of gyration as an indicator of protein structure compactness. *Mol Biol*, 42 (2008) 623.
- 35 Heffernan R, Paliwal K, Lyons J, Dehzangi A, Sharma A, Wang J, Sattar A, Yang Y & Zhou Y, Improving prediction of secondary structure, local backbone angles, and solvent accessible surface area of proteins by iterative deep learning. *Sci Rep*, 5 (2015) 11476.
- 36 Zhang G, Li L, Li J, Li P, Zeng S, Sun H & Li E, Palbociclib triggers apoptosis in bladder cancer cells by Cdk2-induced Rad9-mediated reorganization of the Bak. Bcl-xl complex. *Biochem Pharmacol*, 163 (2019) 133.
- 37 Xu H, Tang Z, Zuo Y, Xiong F, Chen K, Jiang H, Luo C & Zhang H, Molecular dynamics simulation revealed the intrinsic conformational change of cellular inhibitor of apoptosis protein-1. *J Biomol Struct Dyn*, 38 (2020) 975.
- 38 Vila-Julιά G, Granadino-Roldan JM, Perez JJ & Rubio-Martinez J, Molecular Determinants for the Activation/Inhibition of Bak Protein by BH3 Peptides. *J Chem Inf Model*, 60 (2020) 1362.
- 39 Toppo AL, Yadav M, Dhagat S, Ayothiraman S, Jujjavarapu SE, Molecular docking and ADMET analysis of synthetic statins for HMG-CoA reductase inhibition activity. *Indian J Biochem Biophys*, 58 (2021) 127.
- 40 Farmer T, O'Neill KL, Naslavsky N, Luo X & Caplan S, Retromer facilitates the localization of Bcl-xL to the mitochondrial outer membrane. *Mol Biol Cell*, 30 (2019) 1138.
- 41 Yuan L, Liao PP, Song HC, Zhou JH, Chu HC & Lyu L, Hyperbilirubinemia induces pro-apoptotic effects and aggravates renal ischemia reperfusion injury. *Nephron*, 142 (2019) 40.
- 42 Lee S, Lee Y, Kim H, Lee DY & Jon S, Bilirubin nanoparticle-assisted delivery of a small molecule-drug conjugate for targeted cancer therapy. *Biomacromolecules*, 19 (2018) 2270.
- 43 Srivastava P, Hira SK, Srivastava DN, Gupta U, Sen P, Singh RA & Manna PP, Protease-responsive targeted delivery of doxorubicin from Bilirubin-BSA-Capped mesoporous silica nanoparticles against colon cancer. *ACS Biomater Sci Eng*, 3 (2017) 3376.